Chapter 6

Haze Removal: Structural Patch Decomposition Multi-Exposure Image Fusion

6.1 Background

Image dehazing is a severe and challenging problem due to its ill-posed behavior and is highly desired in various vision based applications such as computer vision, image processing, computational photography, remote sensing, outdoor driving assistance, and video surveillance, etc. Image fusion plays a vital role in digital photography, image processing, remote sensing, computer vision, and computational imaging, etc. Its aim is to generate a fusion image by combining the complementary images of input source image. The real-time natural single image captured by camera often suffer with over-exposure or under-exposure problems. The reason behind that is dynamic range of luminance values in the scene span much wider than the

camera can capture it. High-dynamic-range (HDR) imaging techniques overcome this limitation using multiple exposures of image. So, a tone mapping process is required to compress the dynamic range of HDR images to display the scene with low dynamic range (LDR). In computer vision, HDR imaging can be fixed by multi-exposure image fusion (MEF) method. In MEF, a cost effective way is used to solve the dynamic range gap between HDR imaging and LDR displays.

The existing multi-exposure image fusion (MEF) methods perform operations like weight map smoothing, weight calculation, detail enhancement, multi scale implementation, etc. to fuse input images and obtain desired output. Generally, fusion-based image dehazing methods remove haze in two steps: first, it generates multi-exposures from the input hazy image and then, fuses them to restore the desired haze-free image. Generally, most of the existing MEF methods are based on pixel-wise concept. The weighting map used in MEF based methods is often too noisy and hence, if these methods are directly applied for image fusion process, they may generate various artifacts e.g., color cast [29], pseudo-color [32, 97], and glowing effects [98] in the restored image.

To overcome these drawbacks, structural patch decomposition-based multi-exposure image fusion (SPD-MEF) [99] algorithm came in existence. It directly decomposes the multi-exposure images into three independent components such as signal strength, signal structure and signal mean intensity. SPD-MEF algorithm use patch of hazy image instead of individual pixels. Advantages of SPD method in image fusion process and its applications are listed below:

- The SPD-MEF method generates noise free weight map. So, improved visual quality is achieved without any kind of post processing step. This implies that post processing step is inessential.

- It decomposes each color channel independently and natural color information is extracted for the entire patch jointly instead of an individual pixel. Therefore, it provides more natural color information.

- Next, the direction information of signal structure component enables us to easily check the structural consistency of multi-exposure patches so as to produce a high quality image with reduced artifacts.

- The SPD-MEF method consistently produces better quality fused images for static scenes.

- It also provides significant perceptual gains for dynamic scenes while keeping the computational complexity manageable as verified by our complexity analysis and execution time comparison.

In this Chapter, a new effective edge-aware weighting filter-based structural patch decomposition multi-exposure image fusion is proposed for single image dehazing. The rest of the Chapter is structured as follows.

The proposed haze removal algorithm is specified in Section 6.2. Experimental results and analysis are discussed in Section 6.3 and Section 6.4 concludes the Chapter.

6.1.1 Major Contributions of the Work

The main contributions of this work are as follows:

- A structural patch decomposition multi-exposure image fusion (SPD-MEF) algorithm is proposed for single image dehazing.

- A new edge-aware weighting filter is proposed to refine the weight maps of each decomposed image patch accurately. This filter removes halos and over-smoothing effect strongly and preserves edge information precisely in both flat and sharp regions.

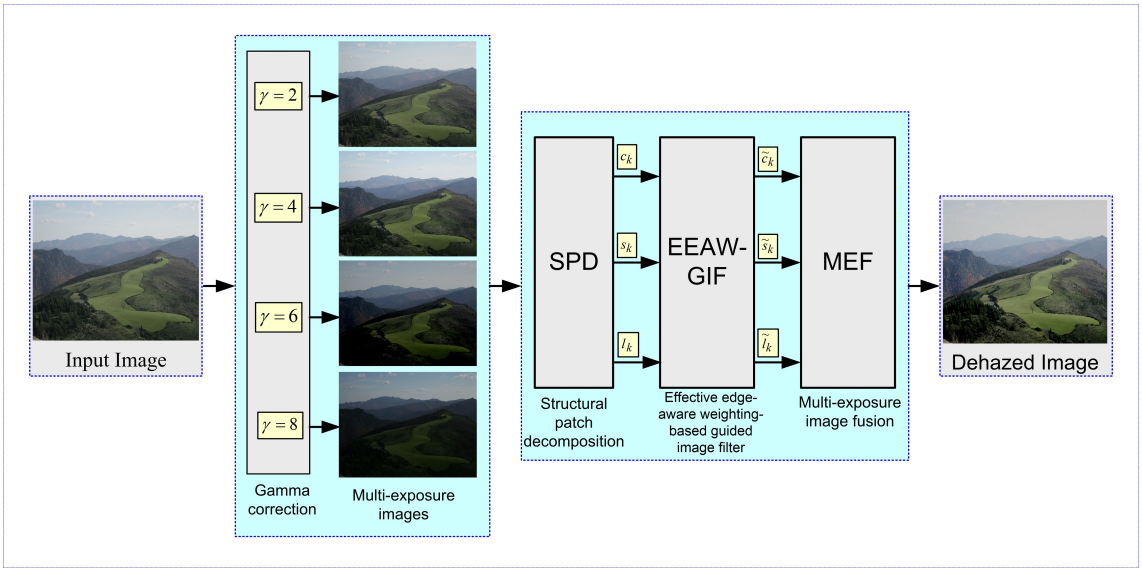

FIGURE 6.1: Flow diagram of the proposed method.

6.2 The Proposed Algorithm

Here, a novel effective edge-aware weighting filter-based robust structural patch decomposition multi-exposure image fusion method is proposed for single image dehazing. The framework of the proposed haze removal method is shown in Figure 6.1. The proposed dehazing method has four main steps as follows:

- In the first step, a set of four gamma coefficients ($\gamma = 2, 4, 6, 8$) is applied on input hazy image and corresponding underexposed images are obtained.

- In the second step, the structural patch decomposition (SPD) method is used to decompose each individual underexposed image into three conceptually independent components namely: signal strength, signal structure, and signal mean intensity.

- In the third step, an effective edge-aware weighting-based guided image filter (EEAWGIF) is proposed to refine the weight maps of each decomposed image patches for effective image dehazing.

- Finally, multi-exposure image fusion (MEF) method is applied to fuse the refined image patches and provide effective dehaze outcomes.

6.2.1 Artificial Exposure by Gamma Correction

The gamma correction method is employed to enhance the local perceptibility of input images by producing multi-exposure images. Multi-exposure images are obtained after applying different gamma coefficients (γ) [21] on input hazy image. When $\gamma < 1$, color tone of high luminance contents exist in the overexposed images. When $\gamma > 1$, it improves contrast and preserves more detail information in the underexposed image. After quantifying the pixel values into a small range, we can obtain the underexposed images of negligible intensity. The following equation can be used to express the contrast of an image for a given area Ω:

$$\ell(\Omega) = I^{\Omega}_{max} - I^{\Omega}_{min}, \tag{6.1}$$

where $I^{\Omega}_{max} = \max\{I(x) \mid x \in \Omega\}$ and $I^{\Omega}_{min} = \min\{I(x) \mid x \in \Omega\}$. Mathematically, gamma correction is expressed as:

$$I_G = \hat{a}.I^{\gamma}, \tag{6.2}$$

where I represents input hazy image, I_G represents gamma corrected image, $\hat{a}$ and γ are two positive real numbers where $\hat{a}$ defaults to 1. Generally, gamma correction can improve the visual quality of hazy image by dynamic range adjustment. The dynamic range is defined as difference between the brightest and darkest intensity values that a camera can register. It can improve the visual quality to a definite extent [21, 32] and it becomes difficult to control the balance between the over-saturation of narrow-range regions and the haze removal of wide-range regions. Generally, visibility of more fine details in wide range regions increases with the increase of gamma correction values, while the visibility of details in near range regions begins to reduce contrast [21]. To prove experimentally, we have applied two set of four gamma coefficients ($\gamma = 2, 3, 4, 5$) and ($\gamma = 2, 4, 5, 7$) on two different real hazy images and their outcomes are shown in Figure 6.2 and Figure 6.3, respectively. It is clear from Figure 6.2-6.3 that as gamma increases ($\gamma > 1$), visibility of fine details in wider range regions (red and yellow highlighted regions in Figure 6.2 and Figure 6.3, respectively) is increases, while the visibility of details in near range regions (magenta and red highlighted regions in Figure 6.2 and Figure 6.3, respectively) begins to reduce contrast. It is clear from multi-exposure images that visibility of hazy image (fine details of mountain, tree and sky regions) increases as gamma coefficient value increases. Therefore, we have used a set of four gamma coefficients γ = (2, 4, 6, 8) to produce the correct underexposed sequences and they represent a range of different levels of contrast. These coefficients provide a better balance between contrast and brightness in the final dehazed image. The coefficient $\gamma = 2$ is suitable for low-contrast scenes, $\gamma = 4$ is suitable for medium-contrast scenes, $\gamma = 6$ is suitable for high-contrast scenes, and $\gamma = 8$ is suitable for very high-contrast scenes. These coefficients help to capture more details and enhance the visibility of the hazy image. The exposure outcomes of input hazy image for four gamma coefficients γ = (2, 4, 6, 8) is shown in Figure 6.4 (b) to 6.4 (e), respectively.

(a) Input 1 (b) $\gamma = 2$ (c) $\gamma = 3$

(d) $\gamma = 4$ (e) $\gamma = 5$

FIGURE 6.2: Processed exposure outcomes for different Gamma correction values.

(a) Input 2 (b) $\gamma = 2$ (c) $\gamma = 4$

(d) $\gamma = 5$ (e) $\gamma = 7$

FIGURE 6.3: Processed exposure outcomes for different Gamma correction values.

(a) Input 3 (b) $\gamma = 2$ (c) $\gamma = 4$

(d) $\gamma = 6$ (e) $\gamma = 8$

FIGURE 6.4: Processed exposure outcomes for different Gamma correction values.

6.2.2 Structural Patch Decomposition-Based Multi-Exposure Image Fusion (SPD-MEF)

The SPD-MEF [99] method is used to decompose an image patch $x_k \in \mathbb{R}^{Cr^2}$ (where C denotes number of color channels and r is the spatial size of image patch) in three conceptually independent components—signal strength, signal structure, and signal mean intensity can be obtained using following relationships:

$$\begin{aligned} x_k &= \|x_k - \mu_{x_k}\| \cdot \frac{x_k - \mu_{x_k}}{\|x_k - \mu_{x_k}\|} + \mu_{x_k} \\ x_k &= \|\tilde{x}_k\| \cdot \frac{\tilde{x}_k}{\|\tilde{x}_k\|} + \mu_{x_k} \\ x_k &= c_k \cdot s_k + l_k, \end{aligned} \tag{6.3}$$

where $\|.\|$ represents l_2 norm, $\tilde{x}_k$ represents patch x that have no mean value (mean-removed patch), μ_{x_k} represents mean value of the patch, c_k represents signal strength,

s_k represents signal structure by unit vector and l_k represents mean intensity at k-th image patch. Due to invertible process of patch decomposition, one can obtain the desired output image patch after fusion of these three components c_k, s_k and l_k. The signal strength of the fused image patch x_k can be denoted as:

$$\hat{c} = \max_{1 \leq k \leq K} c_k = \max_{1 \leq k \leq K} \|\tilde{x}_k\|, \tag{6.4}$$

where K represents total number of multi-exposure image patches and x_k represents the image patch in the k-th image. The signal structure can be represented as:

$$\hat{s} = \frac{\overline{s}}{\|\overline{s}\|}, \text{ and } \overline{s} = \sum_{k=1}^{K} \beta_k s_k, \tag{6.5}$$

where weights $\beta_k \geq 0$ for $k = 1, 2, 3...K$, and $\sum_k \beta_k = 1$. The weight β_k is proportional to $\|\tilde{x}_k\|$ and can be expressed as:

$$\beta_k = \frac{\|\tilde{x}_k\|^p}{\sum_{k=1}^{K} \|\tilde{x}_k\|^p}, \tag{6.6}$$

where $p \geq 0$ is an exponent parameter.

The mean intensity $\hat{l}$ of the local image patch x_k can be denoted as:

$$\hat{l} = \sum_{k=1}^{K} \alpha_k l_k. \tag{6.7}$$

where $\alpha_k \geq 0$ for $1 \leq k \leq K$ is a weighting function of the global mean μ_k and the local mean l_k of the k-th local patch x_k.

Algorithm 2 SPD-MEF Based EEAWGIF for Image Dehazing

Input: Source image I, pixel position (x,y).

1: Calculate I_G for a set of four different gamma coefficient value (γ = 2, 4, 6, 8) and generate multi-exposure images, respectively (via Eq. (6.2)).
2: **for** each underexposed images **do**
3: Using SPD-MEF algorithm, first every underexposed image patch is decomposed into three independent components namely; signal strength $\hat{c}$, signal structure $\hat{s}$ and signal mean intensity $\hat{l}$ by Eq. (6.4), (6.5) and (6.7), respectively.
4: Compute $\hat{c}$, $\hat{s}$ and $\hat{l}$ separately.
5: Refine the weight maps of Base layer α_k and Detail layer β_k of each SPD image patches by a new effective edge-aware weighting ($\overline{\varphi}$) based guided image filter (EEAWGIF).
6: **for** $j = 1$ to $j - 1$ **do**
7: Compute the refined $\tilde{c}(j)$, $\tilde{s}(j)$ and $\tilde{l}(j)$ separately.
8: Reconstruct the fused patches by $\hat{x}_k = \tilde{c}_k \; . \; \tilde{s}_k + \tilde{l}_k$.
9: Aggregate fused patch into $\hat{X}_k$.

Output: Fused dehazed image $\hat{X}$.

6.2.3 Effective Edge-Aware Weighting-Based Guided Image Filter (EEAWGIF)

The SPD-MEF [99] and its improved variant [100, 101] can be directly applied on multi-exposure images to decompose the input hazy image into three independent components namely; signal strength $\hat{c}$, signal structure $\hat{s}$, and signal mean intensity $\hat{l}$ and fused results with high accuracy and efficiency can be achieved. However, halo artifacts and detail loss (blurred edges or noise) still persist in both flat and sharp regions. Therefore, a novel effective edge-aware weighting-based guided image filter (EEAWGIF) is proposed to remove these artifacts. The proposed EEAWGIF refines the weight maps of each decomposed image patches for effective haze removal. In this approach, decomposed mean intensity can be modified and expressed as:

$$l_i = a_k x_i + b_k, \tag{6.8}$$

where i and k are indices, and (a_k, b_k) are two linear coefficients in k-th image patch. The optimal value of a_k and b_k can be obtained by minimizing the difference between x_k and l. It can be expressed as:

$$F(a_k, b_k) = \sum_{k=1}^{K}[(a_k x_k + b_k - x_k)^2 + \varepsilon\overline{\varphi}a_k^2], \tag{6.9}$$

where ε represents the regularization parameter used to penalizes large a_k value and $\overline{\varphi}$ is an effective edge-aware weighting constraint. It can be expressed as:

$$\overline{\varphi}(k) = \frac{\sigma_{k,1}\sigma_{k,r}}{\overline{\sigma}^2}. \tag{6.10}$$

where $\overline{\sigma}^2 = \frac{1}{K}\sum_{k=1}^{K}\sigma_k^2$ is an average variance for all pixels of input image and $\sigma_{k,1}$, $\sigma_{k,r}$ are local variances at radius 1 and r in a k-th patch, respectively. Similar to GIF [49], WGIF [50] and GGIF [51] methods, the computational complexity of $\overline{\varphi}(k)$ is also $O(N)$ for an image with N pixels.

The optimized a_k can be expressed as:

$$a_k = \frac{\sum_{k=1}^{K} x_k^2 - m_k x_k}{\sigma_k^2 + \varepsilon\overline{\varphi}}, \tag{6.11}$$

and b_k can be expressed as:

$$b_k = x_k - m_k a_k, \tag{6.12}$$

where σ_k^2 and m_k are the variance and mean of input patch x_k, respectively.

According to GIF [49],

$$\sum_{k=1}^{K} x_k^2 - m_k x_k = \sigma_k^2, \tag{6.13}$$

and

$$x_k = m_k. \tag{6.14}$$

Substituting (6.13) and (6.14) into (6.11) and (6.12), respectively. Finally, optimized constant coefficients can be expressed as:

$$a_k = \frac{\sigma_k^2}{\sigma_k^2 + \varepsilon\overline{\varphi}}, \tag{6.15}$$

$$\begin{aligned} b_k &= (1 - a_k)m_k \\ b_k &= \frac{\varepsilon m_k \overline{\varphi}}{\sigma_k^2 + \varepsilon\overline{\varphi}}. \end{aligned} \tag{6.16}$$

After substituting a_k and b_k into signal mean intensity l, signal strength c and signal structure s can be expressed as:

$$l = \frac{\sigma_k^2}{\sigma_k^2 + \varepsilon\overline{\varphi}} + \frac{\varepsilon m_k \overline{\varphi}}{\sigma_k^2 + \varepsilon\overline{\varphi}}, \tag{6.17}$$

$$c = \frac{\varepsilon\overline{\varphi}\|x_k - m_k\|}{\sigma_k^2 + \varepsilon\overline{\varphi}}, \tag{6.18}$$

$$s = \frac{(x_k - m_k)}{\|x_k - m_k\|}. \tag{6.19}$$

6.3 Experimental Results and Analysis

The performance of the proposed method is experimented and evaluated using Matlab R2018a on a PC with Intel (R) Core (TM) i7-6700 CPU @ 3.40 GHz of a 64-bit operating system with RAM-8GB. In this experiment, the patch size (N) is fixed 15. The regularization parameter ε and the parameter T [101] are set 0.01 and 1, respectively for effective fusion and image dehazing.

6.3.1 Dataset

The performance of the proposed method is tested on indoor real hazy, outdoor real hazy, indoor synthetic hazy, outdoor synthetic hazy, and nighttime hazy images from various datasets, viz. **D-HAZY** (1400 images) [65], **NYU2** (464 images) [66], **HazeRD** (15 images) [69], **O-HAZE** (45 images) [71], **I-HAZE** (35 images) [70], **NH-HAZE** (55 images) [72], **RESIDE-ITS** (950 images) [73], **RESIDE-OTS** (1100 images) [73], **RESIDE-HSTS** (20 images) [73], **Fattal** (15 images) [16], **Night-time hazy** (20 images) [78] and their results are compared with the 14 existing DCP [15], CAP [17], DSPP [18], CEP [19], BDPK [20], IDBP [23], AMEIF [32], AIFASD [33], FFDHAIP [34], JCEEFID [36], RefineDNet [42], TMSGAN [43], EANet [44], MSAFFNet [45] haze removal methods for effective analysis.

6.3.2 Qualitative Analysis

The proposed method is tested on about 4,119 images using different datasets viz. **D-HAZY** [65], **NYU2** [66], **HazeRD** [69], **O-HAZE** [71], **I-HAZE** [70], **NH-HAZE** [72], **RESIDE-ITS** [73], **RESIDE-OTS** [73], **RESIDE-HSTS** [73], **Fattal** [16], **Night-time hazy** [78] and compared with 14 state-of-the-art haze removal methods out of which DCP [15], CAP [17], DSPP [18], CEP [19], BDPK [20], IDBP [23] are prior based haze removal methods, AMEIF [32], AIFASD [33], FFDHAIP [34], JCEEFID [36] are fusion-based haze removal methods and RefineDNet [42], TMSGAN [43], EANet [44], MSAFFNet [45] are four deep learning-based image dehazing methods. Next, the visual comparisons of the proposed method with 14 existing DCP [15], CAP [17], DSPP [18], CEP [19], BDPK [20], IDBP [23], AMEIF [32], AIFASD [33], FFDHAIP [34], JCEEFID [36], RefineDNet [42], TMSGAN [43], EANet [44], MSAFFNet [45] haze removal methods for indoor real hazy, outdoor

(a) Input (b) DCP (c) CAP (d) DSPP

(e) CEP (f) BDPK (g) IDBP (h) AMEIF

(i) AIFASD (j) FFDHAIP (k) JCEEFID (l) RefineDNet

(m) TMSGAN (n) EANet (o) MSAFFNet (p) The proposed

FIGURE 6.5: Visual comparison of different dehaze methods and the proposed method.

real hazy, indoor synthetic, outdoor synthetic and night-time hazy images are shown in Figure 6.5 to 6.8, respectively. All the benchmark hazy images are tested using the proposed method and dehazed outcomes are compared with the existing haze removal methods. It is clear from these figures that the dehaze outcomes obtained by the existing DCP [15], CAP [17], DSPP [18], CEP [19], BDPK [20], IDBP [23], AMEIF [32], AIFASD [33], FFDHAIP [34], JCEEFID [36], RefineDNet [42], TMS-GAN [43], EANet [44], and MSAFFNet [45] methods removes halo artifacts, over smoothing effectively and preserve edge informations accurately in the flat (smooth)

(a) Input (b) DCP (c) CAP (d) DSPP

(e) CEP (f) BDPK (g) IDBP (h) AMEIF

(i) AIFASD (j) FFDHAIP (k) JCEEFID (l) RefineDNet

(m) TMSGAN (n) EANet (o) MSAFFNet (p) The proposed

FIGURE 6.6: Visual comparison of different dehaze methods and the proposed method.

regions. However, they fail in sharp regions. It is clearly visible from dehazed outcomes that the proposed method removes halo artifacts, over smoothing strongly and preserves edge information more precisely in both flat and sharp regions than the existing DCP, CAP, DSPP, CEP, BDPK, IDBP, AMEIF [32], AIFASD [33], FFDHAIP, JCEEFID, RefineDNet, TMSGAN, EANet, and MSAFFNet haze removal methods.

As observed from Figure 6.5 to 6.8 that IDBP [23], JCEEFID [36], EANet [44], and

(a) Input (b) DCP (c) CAP (d) DSPP

(e) CEP (f) BDPK (g) IDBP (h) AMEIF

(i) AIFASD (j) FFDHAIP (k) JCEEFID (l) RefineDNet

(m) TMSGAN (n) EANet (o) MSAFFNet (p) The proposed

FIGURE 6.7: Visual comparison of different dehaze methods and the proposed method.

MSAFFNet [45] provide promising results for hazy images. But, these methods are incapable of producing similar results for natural hazy and nighttime hazy images whereas, the proposed method is independent of the nature of input image and it performs equally well for all the aforesaid datasets as compared to the existing methods. Finally, it is clear from these figures that the proposed method removes halo effect, over smoothing more strongly and preserve edge information precisely in both flat and sharp regions as compared to the existing methods.

(a) Input (b) DCP (c) CAP (d) DSPP

(e) CEP (f) BDPK (g) IDBP (h) AMEIF

(i) AIFASD (j) FFDHAIP (k) JCEEFID (l) RefineDNet

(m) TMSGAN (n) EANet (o) MSAFFNet (p) The proposed

FIGURE 6.8: Visual comparison of different dehaze methods and the proposed method.

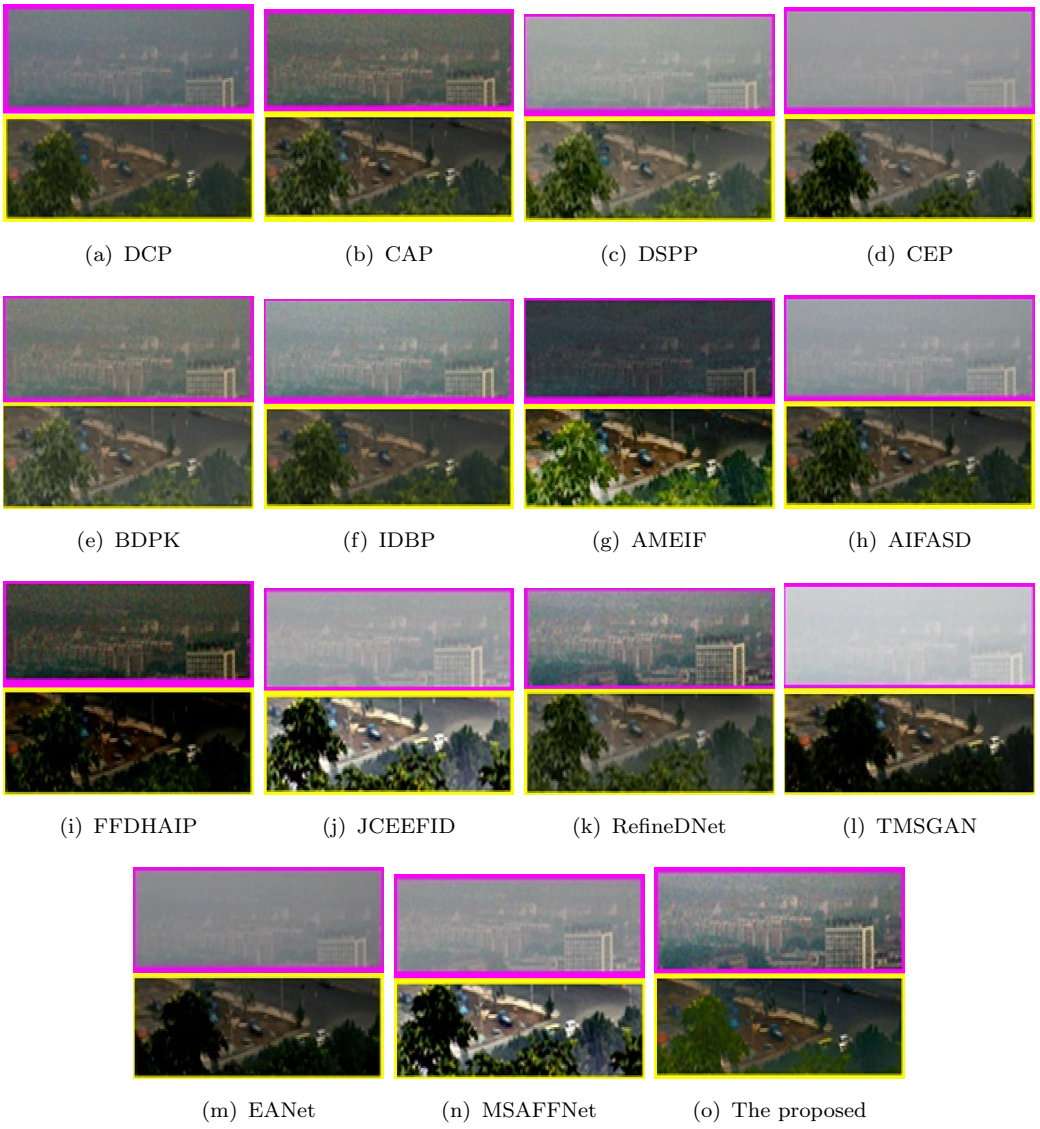

(a) DCP (b) CAP (c) DSPP (d) CEP

(e) BDPK (f) IDBP (g) AMEIF (h) AIFASD

(i) FFDHAIP (j) JCEEFID (k) RefineDNet (l) TMSGAN

(m) EANet (n) MSAFFNet (o) The proposed

FIGURE 6.9: Enlarged Form of Highlighted rectangular portion of the 6.8

6.3.3 Quantitative Analysis

In order to demonstrate the effectiveness of the proposed method than the existing DCP [15], CAP [17], DSPP [18], CEP [19], BDPK [20], IDBP [23], AMEIF [32], AIFASD [33], FFDHAIP [34], JCEEFID [36], RefineDNet [42], TMSGAN [43], EANet [44], MSAFFNet [45] haze removal methods, three full reference image quality assessment (FR-IQA) metrics and three non-reference image quality assessment

(NR-IQA) metrics are evaluated for 11 datasets viz. **D-HAZY** [65], **NYU2** [66], **HazeRD** [69], **O-HAZE** [71], **I-HAZE** [70], **NH-HAZE** [72], **RESIDE-ITS** [73], **RESIDE-OTS** [73], **RESIDE-HSTS** [73], **Fattal** [16], **Night-time hazy** [78]. The peak signal to noise ratio (PSNR) [87], structural similarity index (SSIM) [86], CIEDE2000 [89], contrast gain (C_g) [85] are FR-IQA metrics and fog aware density evaluator (FADE) [81], Blind image quality index (BIQI) [83], Natural image quality evaluator (NIQE) [84] are NR-IQA metrics.

To assess the effectiveness of the proposed algorithm, some of the full reference image quality assessment (FR-IQA) metrics and non-reference image quality assessment (NR-IQA) metrics are calculated for DCP [15], CAP [17], DSPP [18], CEP [19], BDPK [20], IDBP [23], AMEIF [32], AIFASD [33], FFDHAIP [34], JCEEFID [36], RefineDNet [42], TMSGAN [43], EANet [44], MSAFFNet [45] haze removal methods and the proposed method for 11 datasets viz. **D-HAZY** [65], **NYU2** [66], **HazeRD** [69], **O-HAZE** [71], **I-HAZE** [70], **NH-HAZE** [72], **RESIDE-ITS** [73], **RESIDE-OTS** [73], **RESIDE-HSTS** [73], **Fattal** [16], **Night-time hazy** [78] and listed in Table 6.1-6.11, respectively.

In Table 6.1 to 6.11, red and blue bold face values indicate best and second-best score, respectively. It is clear from Table 6.1 to 6.11 that the proposed method has highest PSNR and SSIM scores than the existing methods except second-highest in Table 6.3 for HazeRD dataset. However, EANet [44], MSAFFNet [45] methods scored second and third-highest PSNR and SSIM values, respectively. It is evident from Table 6.1 to 6.11 that the proposed method has scored best CIEDE2000 and contrast gain C_g values than the rest of the methods except MSAFFNet [45] CIEDE2000 value in Table 6.7. Next, it is observed from Table 6.1 to 6.11 that FADE is lower in the proposed method than the existing methods. The best scores

are **0.916**, **1.438**, **1.338**, **1.110**, **1.149**, **1.037**, **1.141**, **0.722**, **1.035**, and **1.391** for **D-HAZY**, **NYU2**, **HazeRD**, **O-HAZE**, **I-HAZE**, **NH-HAZE**, **RESIDE-ITS**, **RESIDE-OTS**, **RESIDE-HSTS**, **Fattal**, and **Night-time hazy** dataset, respectively. The blind image quality index (BIQI) and natural image quality evaluator (NIQE) metrics are used to calculate distortion and naturality of the restored image, respectively. Their lower values indicate less distortion and more naturalness in the restored image. It is evident from Table 6.1 to 6.11 that the proposed method has scored smallest BIQI and NIQE values than existing methods. The best scores of BIQI and NIQE are **12.57, 12.74, 21.95, 21.04, 10.84, 10.06, 11.29, 10.19, 21.09, 11.56, 11.94** and **2.16, 2.62, 2.64, 3.01, 1.87, 2.48, 1.51, 1.83, 2.33, 2.10, 2.90**, respectively for **D-HAZY**, **NYU2**, **HazeRD**, **O-HAZE**, **I-HAZE**, **NH-HAZE**, **RESIDE-ITS**, **RESIDE-OTS**, **RESIDE-HSTS**, **Fattal**, and **Night-time hazy** datasets.

The average running time of the proposed method and the existing DCP [15], CAP [17], DSPP [18], CEP [19], BDPK [20], IDBP [23], AMEIF [32], AIFASD [33], FFD-HAIP [34], JCEEFID [36], RefineDNet [42], TMSGAN [43], EANet [44], MSAFFNet [45] haze removal methods for 55 hazy images (5 images from 11 dataset) having resolution **185×231**, **384×512**, **512×768**, **600×450**, **1600×1200**, and **2592×1944**, respectively is calculated and their comparative outcomes are reported in Table 6.12. In Table 6.12, the red and blue bold face values in each row indicate best and second-best score, respectively. It is clear from Table 6.12 that the proposed method is faster than the other existing methods. Further, the execution time starts increasing with the increase of resolutions, as expected. Next, computational complexity of SPD-MEF is $\mathcal{O}(N^2MK)$, (from (6.3)) where K represents number of input images, M represents number of pixels of input image and N is the spatial size of the local patch. The proposed method has a complexity $\mathcal{O}(MK)$ similar to [36, 100, 101].

TABLE 6.1: Average Performance comparison on D-HAZY dataset

Dehaze Methods	FR-IQA Metrics				NR-IQA Metrics		
	PSNR	SSIM	CIEDE 2000	C_g	FADE	BIQI	NIQE
DCP	23.37	0.825	8.15	0.148	0.894	48.03	12.94
CAP	22.16	0.913	9.55	0.173	0.957	42.90	10.59
DSPP	24.73	0.907	8.34	0.211	0.872	39.24	9.77
CEP	27.14	0.929	6.09	0.247	0.861	36.05	9.45
BDPK	22.16	0.891	9.07	0.199	0.962	45.19	11.06
IDBP	30.85	0.940	2.02	0.325	0.486	24.80	5.94
AMEIF	27.58	0.905	5.71	0.381	0.758	32.86	9.08
AIFASD	32.43	0.927	1.98	0.435	0.713	30.62	8.80
FFDHAIP	**33.06**	0.929	1.87	0.516	0.684	29.53	8.11
JCEEFID	31.17	0.943	1.99	0.563	0.460	22.59	5.15
RefineDNet	30.31	0.934	2.96	**0.695**	0.552	27.18	7.01
TMSGAN	30.69	0.937	2.05	0.586	0.591	26.47	6.53
EANet	31.90	0.949	1.85	0.640	**0.425**	19.74	4.88
MSAFFNet	32.93	**0.955**	**1.73**	0.671	0.451	**16.06**	**3.72**
The Proposed	**34.69**	**0.968**	**1.14**	**0.697**	**0.308**	**12.57**	**2.16**

6.3.4 Ablation Experiment

In this study, we analyzed the effect of edge-preserving factors, regularization parameter ε, and a parameter T [99–101] for dehazing quality and fusion performance. To assess the impact of edge-preserving factors including regularization parameter ε, we first calculated the average SSIM [86], and FADE [81] values with the proposed method on 10 real hazy images from **RESIDE-HSTS** [73] dataset by varying ε and

TABLE 6.2: Average Performance comparison on NYU2 dataset

Dehaze Methods	FR-IQA Metrics				NR-IQA Metrics		
	PSNR	SSIM	CIEDE 2000	C_g	FADE	BIQI	NIQE
DCP	17.91	0.747	13.94	0.186	2.106	46.53	9.77
CAP	22.64	0.769	15.09	0.279	2.297	38.45	8.35
DSPP	23.73	0.785	14.73	0.384	1.944	37.10	8.13
CEP	20.69	0.818	12.48	0.372	1.705	35.81	7.50
BDPK	19.38	0.755	11.62	0.397	2.081	41.29	9.01
IDBP	29.58	0.841	6.05	0.406	0.999	22.68	5.10
AMEIF	24.91	0.796	10.06	0.385	1.683	33.09	7.34
AIFASD	27.16	0.813	8.95	0.471	1.411	32.75	6.98
FFDHAIP	28.51	0.827	7.31	0.508	1.059	30.59	6.51
JCEEFID	29.91	0.842	5.66	0.526	0.976	20.76	4.69
RefineDNet	27.68	0.838	7.74	0.559	0.982	27.42	6.00
TMSGAN	29.37	0.840	6.46	0.527	1.008	26.19	5.72
EANet	30.13	0.844	5.21	**0.593**	**0.939**	16.40	4.66
MSAFFNet	**30.44**	**0.875**	**5.09**	0.578	0.951	**15.90**	**4.05**
The Proposed	**31.08**	**0.899**	**4.19**	**0.605**	**0.916**	**12.74**	**2.62**

TABLE 6.3: Average Performance comparison on HazeRD dataset

Dehaze Methods	FR-IQA Metrics				NR-IQA Metrics		
	PSNR	SSIM	CIEDE 2000	C_g	FADE	BIQI	NIQE
DCP	20.05	0.696	21.94	0.151	3.291	46.94	8.35
CAP	21.51	0.707	18.51	0.208	2.948	42.58	7.89
DSPP	22.74	0.719	17.03	0.247	2.615	41.26	7.64
CEP	22.92	0.724	16.38	0.311	2.539	39.74	7.11
BDPK	23.38	0.753	20.79	0.299	3.101	44.00	8.10
IDBP	23.91	0.782	9.00	0.368	1.689	30.21	3.76
AMEIF	23.97	0.789	14.68	0.432	2.407	38.89	6.25
AIFASD	24.38	0.813	11.07	0.460	2.261	35.40	6.01
FFDHAIP	25.63	0.827	10.83	0.489	2.037	34.15	5.82
JCEEFID	25.90	0.847	8.71	0.541	1.640	28.84	3.52
RefineDNet	27.47	0.871	9.92	0.617	1.821	32.99	5.34
TMSGAN	28.84	0.895	9.15	0.649	1.705	31.57	4.00
EANet	29.12	**0.954**	**8.35**	0.661	1.607	26.01	**3.03**
MSAFFNet	**29.97**	0.909	8.94	**0.685**	**1.586**	**24.50**	3.17
The Proposed	**31.09**	**0.917**	**7.09**	**0.691**	**1.438**	**21.95**	**2.64**

TABLE 6.4: Average Performance comparison on O-HAZE dataset

Dehaze Methods	FR-IQA Metrics				NR-IQA Metrics		
	PSNR	SSIM	CIEDE 2000	C_g	FADE	BIQI	NIQE
DCP	19.09	0.715	26.06	0.307	2.692	49.25	9.25
CAP	21.89	0.735	25.01	0.355	2.473	46.33	8.73
DSPP	22.34	0.747	23.83	0.393	2.217	46.05	8.45
CEP	23.68	0.769	21.75	0.419	2.193	45.62	7.99
BDPK	25.17	0.775	25.37	0.436	2.586	47.71	9.01
IDBP	25.98	0.788	11.11	0.381	1.486	31.24	5.06
AMEIF	27.05	0.791	20.29	0.473	2.074	42.70	7.46
AIFASD	27.47	0.798	17.67	0.433	1.836	40.89	7.11
FFDHAIP	27.97	0.809	15.09	0.476	1.655	37.45	6.75
JCEEFID	28.67	0.829	10.94	**0.499**	1.469	29.00	**3.97**
RefineDNet	28.90	0.845	13.46	0.482	1.694	36.99	6.34
TMSGAN	29.31	0.862	11.38	0.425	1.507	34.52	5.55
EANet	30.85	0.870	**10.03**	0.459	1.425	26.82	4.65
MSAFFNet	**31.00**	**0.880**	10.92	0.486	**1.401**	**24.95**	4.00
The Proposed	**32.74**	**0.899**	**9.85**	**0.501**	**1.338**	**21.04**	**3.01**

TABLE 6.5: Average Performance comparison on I-HAZE dataset

Dehaze Methods	FR-IQA Metrics				NR-IQA Metrics		
	PSNR	SSIM	CIEDE 2000	C_g	FADE	BIQI	NIQE
DCP	21.69	0.750	25.62	0.155	2.407	47.82	8.37
CAP	22.89	0.781	23.75	0.219	2.015	45.17	7.15
DSPP	23.70	0.795	22.05	0.249	1.908	43.78	6.54
CEP	23.93	0.799	21.99	0.337	1.822	41.08	6.28
BDPK	22.12	0.769	24.18	0.297	2.239	45.93	7.69
IDBP	29.18	0.874	13.44	0.366	1.309	18.70	3.41
AMEIF	25.47	0.808	20.37	0.384	1.809	38.69	5.19
AIFASD	25.84	0.816	19.82	0.405	1.756	35.40	5.03
FFDHAIP	26.76	0.827	17.68	0.445	1.702	30.76	4.76
JCEEFID	29.95	0.880	13.08	0.534	1.244	16.91	3.08
RefineDNet	28.00	0.849	15.97	0.651	1.426	27.84	4.12
TMSGAN	28.73	0.858	15.10	0.581	1.385	21.45	3.90
EANet	30.05	0.906	**12.09**	0.688	1.208	15.83	2.05
MSAFFNet	**31.86**	**0.927**	12.96	**0.714**	**1.175**	**12.67**	2.91
The Proposed	**33.70**	**0.949**	**10.59**	**0.720**	**1.110**	**10.84**	**1.87**

TABLE 6.6: Average Performance comparison on NH-HAZE dataset

Dehaze Methods	FR-IQA Metrics				NR-IQA Metrics		
	PSNR	SSIM	CIEDE 2000	C_g	FADE	BIQI	NIQE
DCP	22.18	0.785	23.86	0.103	2.517	49.82	9.51
CAP	23.80	0.809	22.93	0.152	2.411	44.01	8.87
DSPP	24.15	0.817	22.18	0.375	2.383	41.95	8.53
CEP	24.99	0.829	22.00	0.229	2.304	40.38	8.34
BDPK	23.64	0.791	23.05	0.341	2.490	46.30	9.10
IDBP	29.40	0.900	15.24	0.397	1.593	21.05	4.68
AMEIF	25.71	0.840	20.64	0.407	2.195	37.86	7.26
AIFASD	26.31	0.858	20.14	0.456	2.122	34.02	7.03
FFDHAIP	26.85	0.869	19.61	0.518	2.059	31.75	6.95
JCEEFID	29.76	0.903	14.63	0.502	1.511	18.79	4.09
RefineDNet	28.08	0.881	17.99	0.594	1.894	26.91	6.44
TMSGAN	28.94	0.899	17.12	0.628	1.820	23.76	5.37
EANet	**30.91**	**0.948**	11.94	**0.654**	**1.391**	16.40	3.77
MSAFFNet	30.16	0.913	**11.75**	0.649	1.415	**14.99**	**3.50**
The Proposed	**32.48**	**0.945**	**10.09**	**0.685**	**1.149**	**10.06**	**2.48**

TABLE 6.7: Average Performance comparison on RESIDE-ITS dataset

Dehaze Methods	FR-IQA Metrics				NR-IQA Metrics		
	PSNR	SSIM	CIEDE 2000	C_g	FADE	BIQI	NIQE
DCP	24.08	0.739	23.46	0.217	2.539	45.94	8.88
CAP	25.41	0.744	21.89	0.265	2.451	40.21	7.68
DSPP	25.85	0.752	21.33	0.307	2.425	39.35	7.25
CEP	26.73	0.758	20.75	0.351	2.318	35.58	7.01
BDPK	24.97	0.741	22.10	0.299	2.487	42.57	8.19
IDBP	30.86	0.864	14.21	0.382	1.638	18.92	3.78
AMEIF	28.12	0.776	18.40	0.385	2.255	31.75	6.59
AIFASD	28.80	0.783	16.24	0.412	2.117	30.02	6.17
FFDHAIP	29.57	0.790	16.00	0.450	2.084	27.55	5.83
JCEEFID	31.95	0.879	13.35	0.478	1.486	15.41	3.20
RefineDNet	29.91	0.825	15.19	0.521	1.857	23.94	5.46
TMSGAN	30.13	0.856	14.78	0.563	1.805	21.68	4.11
EANet	32.04	0.889	12.76	0.579	1.338	**13.10**	2.98
MSAFFNet	**32.76**	**0.910**	**11.01**	**0.611**	**1.145**	13.97	**2.35**
The Proposed	**33.85**	**0.939**	**11.28**	**0.626**	**1.037**	**11.29**	**1.51**

TABLE 6.8: Average Performance comparison on RESIDE-OTS dataset

Dehaze Methods	FR-IQA Metrics				NR-IQA Metrics		
	PSNR	SSIM	CIEDE 2000	C_g	FADE	BIQI	NIQE
DCP	25.06	0.750	24.90	0.188	2.630	43.98	8.69
CAP	26.81	0.775	22.83	0.231	2.485	40.08	7.90
DSPP	27.13	0.799	22.05	0.268	2.381	40.18	7.53
CEP	27.73	0.802	21.17	0.326	2.207	36.19	7.38
BDPK	25.97	0.762	24.11	0.364	2.558	43.27	8.21
IDBP	31.95	0.888	14.64	0.391	1.615	18.69	3.65
AMEIF	28.19	0.828	19.73	0.400	2.042	31.75	5.85
AIFASD	29.34	0.841	18.68	0.442	1.983	30.69	5.36
FFDHAIP	29.86	0.855	17.25	0.478	1.808	27.58	4.73
JCEEFID	32.00	0.905	14.00	0.534	1.448	16.84	3.38
RefineDNet	30.42	0.868	17.07	0.496	1.735	22.42	4.11
TMSGAN	30.88	0.879	15.80	0.651	1.701	20.76	4.00
EANet	32.48	**0.919**	**12.03**	**0.663**	1.309	13.55	**2.06**
MSAFFNet	**34.62**	0.902	12.25	0.578	**1.257**	**12.70**	2.64
The Proposed	**35.15**	**0.945**	**10.28**	**0.675**	**1.141**	**10.19**	**1.83**

TABLE 6.9: Average Performance comparison on RESIDE-HSTS dataset

Dehaze Methods	FR-IQA Metrics				NR-IQA Metrics		
	PSNR	SSIM	CIEDE 2000	C_g	FADE	BIQI	NIQE
DCP	20.69	0.831	16.52	0.302	1.705	47.05	8.99
CAP	23.84	0.862	12.91	0.364	1.658	44.76	7.64
DSPP	25.05	0.825	15.69	0.271	1.491	41.11	7.13
CEP	26.81	0.839	10.06	0.390	1.403	37.58	6.90
BDPK	24.17	0.849	14.08	0.435	1.772	45.38	8.05
IDBP	27.47	0.900	4.75	0.418	0.945	31.23	4.37
AMEIF	23.72	0.857	9.64	0.479	1.286	36.19	6.51
AIFASD	28.86	0.861	3.55	0.563	1.119	36.00	6.07
FFDHAIP	28.65	0.875	**2.97**	0.526	0.980	34.97	5.75
JCEEFID	28.53	0.911	3.99	0.641	0.886	26.45	3.80
RefineDNet	24.29	0.883	5.13	0.685	0.966	34.12	5.02
TMSGAN	25.15	0.881	5.09	0.702	0.960	31.50	5.96
EANet	**29.99**	**0.911**	4.12	**0.742**	0.901	24.91	4.17
MSAFFNet	28.16	0.903	3.60	0.694	**0.839**	**22.64**	**3.04**
The Proposed	**29.09**	**0.935**	**3.16**	**0.750**	**0.722**	**21.09**	**2.33**

TABLE 6.10: Average Performance comparison on Fattal dataset

Dehaze Methods	FR-IQA Metrics				NR-IQA Metrics		
	PSNR	SSIM	CIEDE 2000	C_g	FADE	BIQI	NIQE
DCP	23.78	0.775	22.20	0.117	2.307	46.02	9.88
CAP	25.11	0.807	21.05	0.136	2.069	43.85	8.86
DSPP	27.39	0.818	20.77	0.289	1.988	41.16	8.40
CEP	27.94	0.825	20.43	0.257	1.805	40.67	7.98
BDPK	24.52	0.792	21.94	0.345	2.118	44.79	9.21
IDBP	31.44	0.878	14.64	0.404	1.351	22.40	4.83
AMEIF	28.73	0.844	18.85	0.473	1.589	36.31	7.35
AIFASD	29.05	0.856	18.10	0.462	1.552	34.90	6.81
FFDHAIP	29.91	0.859	16.56	0.508	1.487	31.22	6.02
JCEEFID	32.07	0.884	14.03	0.553	1.257	18.53	4.00
RefineDNet	30.14	0.866	15.97	0.604	1.425	30.16	5.79
TMSGAN	30.85	0.872	15.25	0.574	1.386	26.86	5.20
EANet	32.96	**0.890**	12.55	**0.659**	1.239	**13.78**	3.66
MSAFFNet	**33.13**	0.876	**11.89**	0.611	**1.160**	14.99	**2.72**
The Proposed	**33.70**	**0.915**	**9.75**	**0.664**	**1.035**	**11.56**	**2.10**

TABLE 6.11: Average Performance comparison on Night time hazy dataset

Dehaze Methods	FR-IQA Metrics				NR-IQA Metrics		
	PSNR	SSIM	CIEDE 2000	C_g	FADE	BIQI	NIQE
DCP	20.91	0.728	20.59	0.089	2.908	46.90	9.37
CAP	21.70	0.743	18.29	0.097	2.781	41.39	8.76
DSPP	23.05	0.750	17.75	0.116	2.510	40.11	8.49
CEP	24.44	0.759	17.02	0.143	2.384	36.85	8.04
BDPK	21.39	0.735	18.86	0.105	2.825	44.78	9.10
IDBP	30.14	0.843	12.83	0.218	1.935	18.53	4.29
AMEIF	26.73	0.783	15.99	0.274	2.293	31.20	6.99
AIFASD	26.94	0.791	15.46	0.320	2.215	27.14	6.12
FFDHAIP	27.88	0.800	14.87	0.355	2.107	24.66	5.83
JCEEFID	30.59	0.868	11.94	0.379	1.818	17.40	4.15
RefineDNet	29.20	0.825	14.05	0.413	2.055	21.73	5.44
TMSGAN	29.91	0.839	14.01	0.438	1.971	20.15	5.10
EANet	**32.97**	**0.895**	11.30	**0.457**	1.709	15.33	3.89
MSAFFNet	30.05	0.871	**10.75**	0.422	**1.557**	**12.85**	**3.52**
The Proposed	**33.24**	**0.907**	**9.92**	**0.468**	**1.391**	**11.94**	**2.90**

TABLE 6.12: Average Execution time comparison of state-of-the-art methods

Methods	185×231	384×512	512×768	600×450	1600×1200	2592×1944
DCP	4.97	11.81	31.09	49.70	57.18	71.08
CAP	6.03	13.45	40.54	53.92	59.76	72.19
DSPP	5.16	10.82	28.43	45.17	52.60	65.79
CEP	3.10	10.15	23.10	42.59	49.71	63.90
BDPK	2.75	9.19	20.87	38.04	49.85	60.45
IDBP	2.37	8.25	17.55	35.18	46.11	60.12
AMEIF	2.99	6.86	15.40	30.99	42.93	52.28
AIFASD	1.66	6.49	14.96	29.46	42.07	50.11
FFDHAIP	1.48	6.05	14.02	28.70	40.43	48.15
JCEEFID	1.10	5.71	13.76	28.19	37.99	44.00
RefineDNet	0.99	3.97	11.00	23.15	33.05	40.96
TMSGAN	0.90	3.53	9.12	20.65	32.25	36.24
EANet	**0.57**	3.11	**8.07**	18.87	30.16	**34.46**
MSAFFNet	0.79	**2.87**	**8.07**	**16.71**	**25.04**	35.79
The proposed	**0.33**	**2.09**	**5.85**	**11.49**	**20.78**	**26.51**

TABLE 6.13: Impact of regularization parameter ε and T on SSIM and FADE

Metrics	$\varepsilon = 0.25$					$T = 1$				
	T=0.1	T=0.3	T=0.4	T=0.6	T=0.8	ε=0.06	ε=0.18	ε=0.26	ε=0.35	ε=0.43
SSIM	0.873	0.921	0.945	0.967	**0.984**	0.910	0.936	0.957	0.968	**0.980**
FADE	1.393	1.204	1.151	1.119	**1.073**	1.602	1.375	1.196	1.121	**1.065**

T and results of two sets are furnished in Table 6.13. In the first set, we fixed the regularization parameter $\varepsilon = 0.25$ and varied $T = 0.1$, 0.3, 0.4, 0.6 and 0.8, while in second set, we fixed parameter $T = 1$ and varied $\varepsilon = 0.06$, 0.18, 0.26, 0.35, and 0.43, respectively. It is observed from Table 6.13 that value of SSIM increases with increasing of ε and T value. On the other side, it can achieves highest SSIM for higher ε and T value. Here, FADE metric is used to show the effectiveness of the proposed method in hazy conditions. It is evident from Table 6.13 that the average score of FADE is higher for small ε and T value, while it achieves lower score for

high ε and T value.

6.4 Conclusion

In this Chapter, an effective edge-aware weighting filter-based structural patch decomposition multi-exposure image fusion method is presented for single image dehazing. The proposed work removes halo artifacts and over smoothing strongly and preserves edge information precisely in both flat and sharp regions than the existing DCP, CAP, DSPP, CEP, BDPK, IDBP, AMEIF, AIFASD, FFDHAIP, JCEEFID, RefineDNet, TMSGAN, EANet, and MSAFFNet haze removal methods. The proposed work is experimented on about 4,119 images of **D-HAZY**, **NYU2**, **HazeRD**, **O-HAZE**, **I-HAZE**, **NH-HAZE**, **RESIDE-ITS**, **RESIDE-OTS**, **RESIDE-HSTS**, **Fattal**, and **Night-time hazy** datasets. The qualitative analysis proves that the proposed method is independent of the nature of image and it performs equally well for all datasets as compared to the existing dehaze methods. The quantitative analysis shown in Table 6.1 to 6.12 proves that the proposed method performs better than the existing methods. In the quantitative analysis, we calculated PSNR, SSIM, CIEDE2000 as a full reference- and FADE, BIQI, NIQE as non reference- image quality assessment metrics for effective analysis of the proposed work. Results of average execution time, listed in Table 6.12 also demonstrate that the proposed method requires less processing time and it is faster than the existing methods for a given resolution of images. Overall, it can be concluded that the proposed method removes halo artifacts strongly and preserves edge information more accurately than the existing DCP [15], CAP [17], DSPP [18], CEP [19], BDPK [20], IDBP [23], AMEIF [32], AIFASD [33], FFDHAIP [34], JCEEFID [36], RefineDNet [42], TMSGAN [43], EANet [44], MSAFFNet [45] haze removal methods.